Gap junction permeability is diminished in proliferating vascular smooth muscle cells

DAVID T. KURJIAKA, TIMOTHY D. STEELE, MARY V. OLSEN, AND JANIS M. BURT
Department of Physiology, University of Arizona, Tucson, Arizona 85724

Kurjiaka, David T., Timothy D. Steele, Mary V. Olsen, and Janis M. Burt. Gap junction permeability is diminished in proliferating vascular smooth muscle cells. *Am. J. Physiol.* 275 (*Cell Physiol.* 44): C1674–C1682, 1998.—In atherosclerosis and hypertension, vascular smooth muscle cells (SMCs) are stimulated to proliferate and exhibit enhanced gap junction protein expression. Our goal was to determine whether gap junction function differs in proliferating vs. growth-arrested SMCs. A7r5 cells (embryonic rat aortic SMCs) did not proliferate in media with reduced serum (~90% of cells in G_0/G_1 phase after 48–96 h in 1% fetal bovine serum). Dye coupling was less but electrical coupling was comparable in proliferating vs. growth-arrested A7r5 cells, suggesting differences in junctional permselectivity. In growth-arrested cells, junctional conductances measured with potassium glutamate, tetraethylammonium chloride, and KCl were well predicted by the conductivities of these solutions. In contrast, junctional conductances measured with potassium glutamate and tetraethylammonium chloride in proliferating cells were significantly greater than predicted by the conductivities of these solutions. These results suggest that junctions between growth-arrested cells are permeated equally well and simultaneously by anions and cations, whereas junctions between proliferating cells are poorly permeated by large molecules of either charge and equally well but not simultaneously by small anions and cations. The data indicate that A7r5 cells regulate chemical coupling independent of electrical coupling, a capacity that could facilitate growth control while protecting vasomotor responsiveness of vessels.

connexon; intercellular communication; permselectivity; cell cycle; growth control

GAP JUNCTION PROTEINS (connexins, Cx) are present in the cell membrane as hexameric hemichannels. Hemichannels between neighboring cells dock to form the functional channel, which provides a pathway for the diffusive movement between cells of ions, metabolites, and second-messenger molecules (10, 33). In the vasculature, intercellular communication likely functions in a dual role, coordinating vasomotor responses (11, 31, 32) and regulating cell growth (23, 42). Two scenarios relating cell growth and gap junction function have been advanced: one links enhanced growth with reduced or absent communication (23); the other links enhanced growth with elevated expression of connexin proteins and presumably increased coupling (5, 6, 16, 20).

Vascular wall cells appear to fit the second scenario, wherein increased cell growth and proliferation are associated with increased expression of connexin proteins. Proliferation of vascular cells in the adult animal occurs in response to physiological stimuli, leading to angiogenesis, and in response to pathophysiological stimuli, leading to wall thickening or plaque formation, as in hypertension and atherosclerosis, respectively. Comparatively little is known about gap junction protein expression or channel function in the angiogenic setting, but it is apparent in the pathophysiological setting that changes in gap junction expression occur. Smooth muscle cells (SMCs) from hypertensive animals placed in cell culture exhibit a significantly greater gap junctional area per cell than their nonhypertensive counterparts (15). Recent evidence supports and extends this observation by demonstrating increased expression of Cx43 in vivo in aortic smooth muscle of hypertensive animals (16, 35). Similarly, in the early stages of atherogenesis, Cx43 expression in intimal smooth muscle is enhanced (6). These studies did not examine the functional properties of gap junctions between SMCs, nor did they look for expression of Cx40, a gap junction protein coexpressed with Cx43 in SMCs of resistance vessels (22), large arteries (4), and possibly diseased vessels (25) or vessels undergoing vasculogenesis (24). Consequently, the functional ramifications of these changes in connexin expression are unknown.

A number of investigators have reported altered gap junction function in cells stimulated to proliferate with growth factors. Whereas several groups have reported decreased Lucifer yellow dye coupling in cells stimulated to proliferate (21, 29), other groups have reported increased dye coupling and connexin expression (12, 28, 30). The opposite character of the results in these reports could reflect temporal differences, or they could be indicative of cell-specific differences in coupling. Regardless, the dye-coupling technique provides only limited information about gap junction function. For example, a decrease in Lucifer yellow dye coupling could be indicative of *1*) a decreased number of functional channels with no change in their overall permselectivity, *2*) a selective decrease in anion permeability, *3*) a selective decrease in large molecule permeability, or even *4*) a selective decrease in cation permeability that also reduces, to a more limited extent, anion permeability. The implications of these scenarios for the types of molecules that are shared between cells and their importance in the regulation of proliferation and maintenance of normal vasomotor responsiveness of vessels could be quite different.

The purpose of the present study was to determine whether gap junction function differed in proliferating vs. growth-arrested SMCs. A7r5 cells, an embryonic rat aortic SMC line, were selected for these studies, be-

The costs of publication of this article were defrayed in part by the payment of page charges. The article must therefore be hereby marked "*advertisement*" in accordance with 18 U.S.C. Section 1734 solely to indicate this fact.

cause they express the connexins found in SMCs of resistance vessels, Cx40 and Cx43 (22). Proliferating A7r5 cells were found to be less well dye coupled than their growth-arrested counterparts. Despite reduced dye coupling, electrical coupling (measured with KCl patch solution) between proliferating and growth-arrested cells was comparable. Permselectivity studies indicate that gap junctions in proliferating cells are poorly permeated by large molecules (anions or cations), whereas in growth-arrested cells such molecules permeated the junction freely and in accord with their mobilities in bulk solution. The data indicate that gap junctions in SMCs undergo changes in permselectivity as a function of growth status, i.e., changes that would not be expected to compromise their capacity to share electrical signals but would significantly reduce their ability to mediate exchange of larger molecules with growth-regulatory potential.

MATERIALS AND METHODS

Cell culture. A7r5 cells were obtained from American Type Culture Collection at *passage 11* and maintained in DMEM (Sigma Chemical) supplemented with 10% fetal bovine serum (FBS) and antibiotics (5% streptomycin and 3% penicillin) in a humidified, 10% CO_2 incubator at 37°C. Cells were passaged weekly with 0.25% trypsin in Ca^{2+}-Mg^{2+}-free PBS. In several experiments, lipoprotein-free serum (LPD-FBS) was used, thereby eliminating potential mitogenic effects of low-density lipoproteins. Lipoproteins were removed from the serum by gradient centrifugation (17, 18).

Growth curves. Cells were plated at a density of 0.5×10^4 cells/cm^2 in 24-well plates and maintained for 24 h in DMEM containing 10% FBS to allow cells to adhere to the plate and recover from trypsinization. Growth curves were initiated at the end of this recovery period as follows. After cells were washed gently with PBS, cells were maintained for the duration of the growth curve experiment in DMEM containing 10% FBS, 10, 5, 1, or 0.1% LPD-FBS, or 0.1% BSA. Wells were washed daily with PBS, and fresh medium was restored. Every 24 or 48 h, three wells of cells in each treatment group were washed twice with PBS and fixed with 1% glutaraldehyde. Fixed cells were then washed with and stored in PBS until all wells in the experiment had been fixed. On the final day of the growth curve experiment, PBS was removed from all wells, and the fixed cells were incubated in 0.1% crystal violet for 40 min. Cells were then washed with water, dried, and dissolved in 2 ml of 10% acetic acid. The absorbance of the resultant solution, which is linearly related to cell number (data not shown), was determined spectrophotometrically at 590 nm with 10% acetic acid as a blank. Despite identical procedures, data from different experiments are not directly comparable because of variability in final plating density (density 24 h after plating) and staining efficiency, both of which can alter the position of the growth curves relative to the axes, despite identical growth rates. Thus the technique is ideally suited to identifying growth-inhibitory conditions but not to assessing relative rates of growth.

Cell cycle analysis. Fluorescence-activated cell sorting (FACS) was used to quantify the proportion of cells in G_0/G_1, S, and G_2/M phases. A7r5 cells (*passages 18–20*) were plated at low or high density ($\sim 0.5 \times 10^4$ or $\sim 1.5 \times 10^4$ cells/cm^2) on gelatin-coated or uncoated six-well plates and maintained in 10% FBS-DMEM for 24 h. The cells were then washed three times with PBS and subsequently incubated in 0.1% BSA-DMEM, 1% FBS-DMEM, or 10% FBS-DMEM (each treatment at each time point was performed in triplicate). As in the growth curve experiments, to minimize effects of any autocrine growth factors, the medium was changed daily after three washes in PBS (14, 27, 41).

Cells were harvested for cell cycle analysis by using a modification of the procedure from Vindelov and Christensen (38). Briefly, cells were washed three times with PBS and incubated with gentle rocking for 15 min at room temperature in a solution containing trypsin (30 μg/ml), Nonidet P-40 (0.1% vol/vol), and spermine tetrahydrochloride (1.5 mM). After addition of trypsin inhibitor (50 μg/ml) and RNase A (100 μg/ml) to each well, cells were incubated for an additional 15 min at room temperature with gentle rocking. Cells were stained with propidium iodide (400 μg/ml) and filtered through a 50-μm nylon mesh, and their DNA content was quantified on a FACStar flow cytometer within 3 h of harvesting. Cell cycle data were analyzed for the proportion of cells in each stage of the cell cycle by using the WinMDI program.

Dye coupling. A7r5 cells were plated on glass coverslips and grown to confluence. They were then treated with 10 or 1% FBS for 48 h (with PBS washes at 24 h). Coverslips were mounted in a chamber and bathed in Hanks' buffered saline solution. Electrodes with resistances of ~15 MΩ were fabricated (Sutter Instruments) from thin-walled glass (1.0 mm; Corning 6150, AM Systems). The tips of these electrodes were filled with Lucifer yellow (5% in water, ~150 mM), and the remainder of the electrode was backfilled with 150 mM LiCl. An electrode was positioned on the surface of the desired cell, such that it "dented" the membrane. The capacitance compensation feature of the amplifier (model KS-700, WPI) was then overcompensated, which resulted in cell impalement and simultaneous efflux of dye from the electrode into the cell. The electrode was removed from the cell immediately after impalement, and 5 min later the number of neighboring cells to which the dye had diffused was visually determined.

Junctional conductance and permeability. For dual whole cell voltage-clamp experiments, A7r5 cells were plated at low density ($0.4–0.5 \times 10^4$ cells/cm^2) onto glass coverslips coated with 1% gelatin in PBS and maintained in 10% FBS-DMEM for 24 h. On the following day, some of the cells were used for determination of junctional conductance (g_j); these cells composed the proliferating cell group. The remaining cells were washed three times with PBS and subsequently incubated in growth-arrest medium (1% FBS-DMEM) for 48 h (with PBS washes at 24 h). After 48 h in growth-arrest medium, g_j of the cells was determined; these cells composed the growth-arrested cell group.

The dual whole cell voltage-clamp method was used to determine g_j in proliferating and growth-arrested A7r5 cells. Coverslips with proliferating or growth-arrested cells were placed in an experimental chamber and bathed in extracellular solution containing (in mM) 142.5 NaCl, 4 KCl, 1 $MgCl_2$, 5 glucose, 2 sodium pyruvate, 10 HEPES, 15 CsCl, 10 tetraethylammonium chloride (TEACl), 1 $BaCl_2$, and 1 $CaCl_2$; pH and osmolarity were adjusted to 7.2 and 322 mosM, respectively. Patch pipettes were filled with KCl, potassium glutamate (KGlut), or TEACl (PS-KCl, PS-KGlut, or PS-TEACl; Table 1) and fabricated (1.2-mm glass; Corning 6020, AM Systems) such that, irrespective of patch solution, they had resistances of ~8 MΩ. The pH and osmolarity of these solutions were adjusted with KOH (TEA hydroxide for PS-TEACl) and water, respectively; the amount of base and water added to each solution was carefully noted, such that the final salt content of the solution (Table 1) could be calculated. The conductivities (model 2052, VWR) of the three patch solutions were also quantified (Table 1). Solutions were filtered (0.22 μm) before storage and again immediately before use.

Table 1. *Ionic composition of patch pipette solutions*

	PS-KGlut	PS-KCl	PS-TEACl
KCl	0	124	0
KGlut	131	0	0
CsCl	14	14	15
HEPES	10	9	10
EGTA	10	9	10
$CaCl_2$	0.5	0.5	0.5
Glucose	5	5	5
TEACl	10	9	135
$MgCl_2$	3	3	3
Na_2ATP	5	5	5
pH	7.2	7.2	7.2
Osmolarity, mosM	322	322	323
Conductivity, mS/cm	11.75	15.97	10.77

Values are mmol/l unless otherwise noted. PS, patch pipette solution; KGlut, potassium glutamate; TEACl, tetraethylammonium chloride.

Each cell of a pair was patched in the whole cell configuration and voltage clamped (Axopatch 1D) at 0-mV holding potential. Series resistance (R_s) and whole cell capacitance of each cell were determined using these features of the amplifiers; nonjunctional resistances (R_m) were also noted. Command pulses of −10 mV were applied alternately to each cell, and current was recorded from both cells. Junctional current was measured in the unstimulated cell and used to calculate g_j ($I/V = G$, where I is current, V is voltage, and G is conductance). To minimize the effects of R_s and R_m on measurement of g_j, we restricted our analysis of g_j to cell pairs in which R_s was 20–35 MΩ and R_m was >500 MΩ. Under these conditions of R_s and R_m, we underestimate g_j by ~50% (37, 40). However, because mean values for R_s and R_m did not differ for any of the groups reported here, this underestimate is uniform across groups. As a consequence, any differences in g_j between groups that are significant would remain significant after correction for effects of R_s and R_m on the measurement of g_j (37, 40). To minimize possible differences between cultures, cells from the same parental culture were used for the proliferating and growth-arrest groups. Additionally, g_j was measured with PS-KCl and either PS-KGlut or PS-TEACl in an alternating fashion on any given day.

Statistical analysis. Values are means ± SE. Student's *t*-test was employed to compare proliferating with growth-arrested cells tested via dye coupling. Significance was set at $P \leq 0.05$. For the permselectivity data derived with the three patch solutions, data were also compared with *t*-test. However, the Bonferroni adjustment was used to account for multiple comparisons on the same data. This adjustment involves creating a conservative family-wide error rate of $P \leq 0.05$ by dividing 0.05 by the number of comparisons and using that value to determine significance for each comparison.

RESULTS

Growth arrest. To establish conditions that reproducibly arrested A7r5 cell proliferation, the dependence of proliferation on serum content of the growth medium was evaluated. Cell number as a function of time was determined for cells maintained in media containing 0.1, 1, 5, and 10% LPD-FBS, 0.1% BSA, or 10% FBS. Despite reports to the contrary (2, 3), the results (Fig. 1) suggested that 1% FBS was sufficient to produce growth arrest. To further verify this finding, we tested the effects of 1% LPD-FBS on proliferation over a period of 15 days. Figure 2 shows that A7r5 cells do not proliferate in 1% LPD-FBS medium.

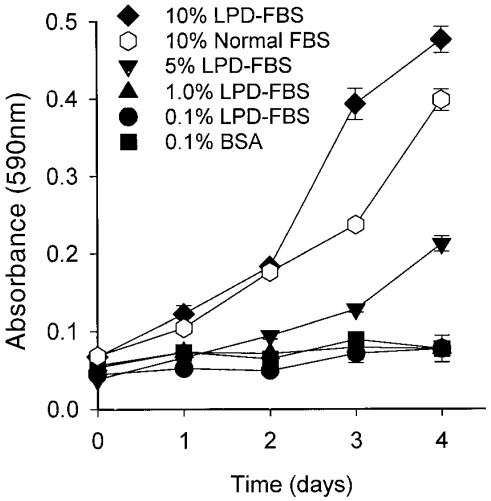

Fig. 1. A7r5 cells fail to proliferate in media with reduced serum content. Cell number was approximated by determining absorbance after cell staining with crystal violet. When serum content was ≤1%, no proliferation occurred. LPD, lipoprotein free; FBS, fetal bovine serum.

Cell cycle analysis. FACS was used to assess where in the cell cycle A7r5 cells arrested and to verify that 1% FBS (vs. the 1% LPD-FBS used in the experiments described above) also produced growth arrest (experimental paradigms are summarized in Table 2). Figure 3 shows the results of an FACS experiment in which the cells were plated at high density and maintained in 10% FBS for 96 h (*A*) or at low density and maintained in 1% FBS for 48 h (*B*). In 10% FBS, 79% of cells were in the G_0/G_1 phase, 6% in the S phase, and 15% in the G_2/M phase. In contrast, 91% of cells cultured for 48 h in 1% FBS were in the G_0/G_1 phase, 5% in the S phase, and 4% in the G_2/M phase. Data from multiple experi-

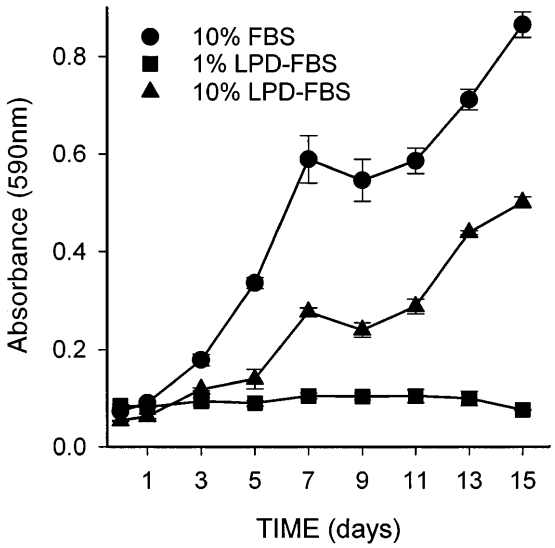

Fig. 2. Proliferation of A7r5 cells was inhibited for extended periods when media contained only 1% LPD-FBS. Apparent partial inhibition by 10% LPD-FBS vs. 10% FBS was not routinely observed and may reflect a different initial seed density.

Table 2. *Experimental paradigms*

Experimental Paradigm	Plating Density, cells/cm^2	Treatment Medium (in DMEM)	Time to Analysis*
Growth curves	0.5×10^4†	10% FBS	0–15 days
		0.1% BSA	0–15 days
		0.1–10% LPD-FBS	0–15 days
Cell cycle analysis	0.5×10^4†‡ or	10% FBS	48 and 96 h
	1.5×10^4†‡§	1% FBS	48 and 96 h
		0.1% BSA	48 and 96 h
Dye coupling	1.5×10^4†§	10% FBS	48 h
		1% FBS	48 h
Junctional conductance and permselectivity	$0.4–0.5\times10^4$‡	10% FBS	0 h
		1% FBS	48 h

FBS, fetal bovine serum; LPD, lipoprotein free. *All experimental paradigms included a 24-h period after plating, during which cells recovered from trypsinization and adhered to substrate. This 24-h period is not included in time to analysis. †Without gelatin. ‡With gelatin. §Confluent density.

ments in which the effects of 1% FBS and 0.1% BSA on cell cycle position were assessed on cells plated at low or high density for 48 or 96 h, respectively, are summarized in Fig. 4. The data indicate that cells plated at low or high density and arrested in 1% FBS vs. 0.1% BSA for 48 or 96 h were not different. In addition, no effect of gelatin coating could be detected (data not shown).

Dye coupling. To determine whether gap junction function differed in proliferating vs. growth-arrested A7r5 cells, the number of neighboring cells to which intracellularly injected Lucifer yellow diffused was measured. After A7r5 cells achieved confluence, the medium bathing the cells was changed to 1% FBS to induce growth arrest or 10% FBS to maintain the proliferative state. After 48 h, Lucifer yellow was injected into individual cells and the extent of dye coupling was assessed. As illustrated in Fig. 5, growth-arrested A7r5 cells (in 1% FBS) were fivefold better coupled than proliferating cells (in 10% FBS).

Junctional conductance. The dual whole cell voltage-clamp technique offers a more quantitative measure of cell-cell coupling. Consequently, this technique was used to assess g_j in proliferating and growth-arrested A7r5 cells. Contrary to expectations arising from the dye-coupling experiments, g_j (measured with PS-KCl) between proliferating cells (10% FBS) was not different (Fig. 5) from g_j between arrested cells (1% FBS). Reconciliation of these electrical-coupling results with the dye-coupling results prompted us to investigate possible differences in permselectivity of the junctions in proliferating vs. growth-arrested cells.

Macroscopic junctional selectivity. To determine whether junctional permselectivity differed in growth-arrested vs. proliferating cells, we measured g_j with patch solutions that differed in the composition of primary current-carrying ions (Table 1). Substitution of $Glut^-$ for Cl^- distinguishes the PS-KGlut solution from PS-KCl; comparison of g_j values measured with these solutions allows determination of anion permeability. Substitution of TEA^+ for K^+ distinguishes the PS-TEACl solution from PS-KCl; comparison of g_j values measured with these solutions allows determination of cation permeability. Because of differences in the mobilities of the constituent ions, the conductivities of these solutions differed as summarized in Table 1.

As shown in Fig. 5, with PS-KCl, growth-arrested and proliferating cells exhibited nearly identical levels of coupling (Table 3). In growth-arrested cells, g_j values measured with PS-KGlut or PS-TEACl were well predicted by the differences in bulk conductivities of the respective patch solutions (Table 3, Fig. 6). Thus the conductivity of PS-KGlut was 74% of that measured with PS-KCl, and g_j in growth-arrested cells measured

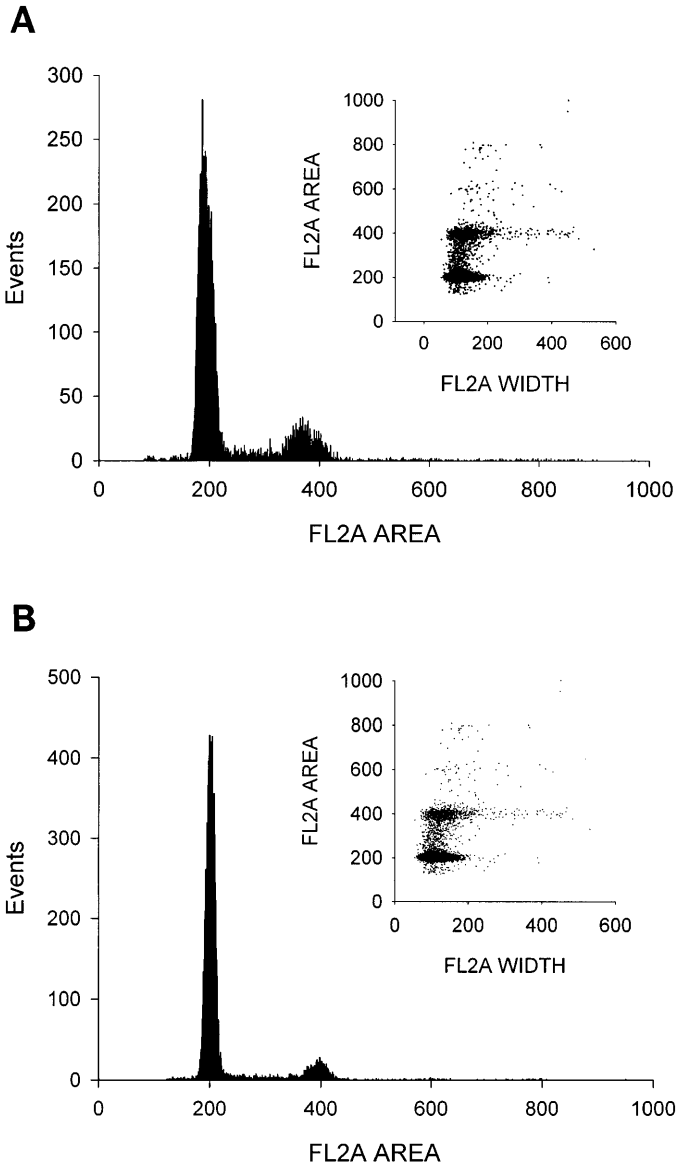

Fig. 3. DNA content of proliferating (*A*) vs. growth-arrested (*B*) A7r5 cells as determined by fluorescence-activated cell sorting of propidium iodide-stained cells. Approximately 79% of cells reside in G_0/G_1 phase of cell cycle (tallest peak) for proliferating cells vs. 91% for growth-arrested cells. *Insets*: actual distributions of 10,000 cells counted. Cells in G_0/G_1 phase are found in bottom cluster of points, cells in G_2/M phase in top cluster, and cells in S phase between top and bottom clusters. Note substantial reduction in cells in S and G_2/M phases in growth-arrested population.

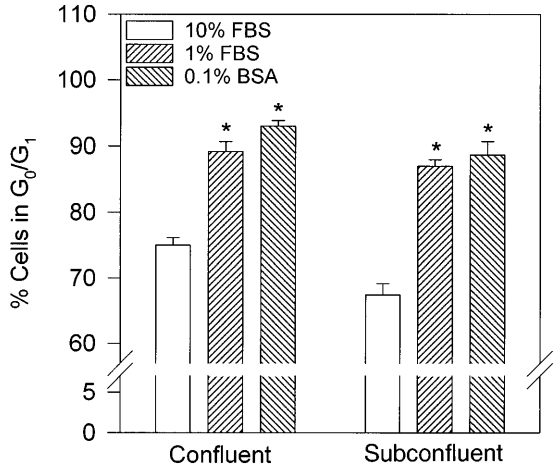

Fig. 4. Cell cycle distribution of subconfluent (48 h) and confluent (96 h) A7r5 cells in 10 or 1% FBS and 0.1% BSA. Approximately 75% of cells in 10% FBS reside in G_0/G_1 phase, irrespective of plating density, whereas ~90% of cells in 1% FBS or 0.1% BSA reside in G_0/G_1 phase, irrespective of plating density. Sample sizes were 18, 12, and 18 for confluent cells (10% FBS, 1% FBS, and 0.1% BSA, respectively) and 5, 6, and 6 for subconfluent cells (10% FBS, 1% FBS, and 0.1% BSA, respectively). *Significantly different from 10% FBS.

with PS-KGlut was 73% of that measured with PS-KCl. Similarly, with PS-TEACl, g_j in the growth-arrested cells was 72% of that measured with PS-KCl vs. the predicted difference of 67%. These data suggest that in the growth-arrested cells *1*) anions and cations contribute simultaneously to junctional current, *2*) K^+, Cl^-, $Glut^-$, and TEA^+ permeate the channel, and *3*) the contribution of these ions to junctional current is well predicted by their mobilities in bulk solution.

In direct contrast to the data obtained on growth-arrested cells, in proliferating cells, g_j values measured with the various patch solutions were significantly

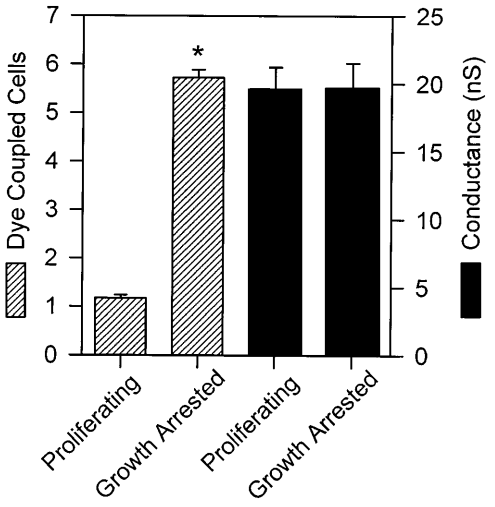

Fig. 5. Proliferating A7r5 cells exhibited reduced dye coupling (1.17 ± 0.06 vs. 5.725 ± 0.16 cells, $n = 40$ for both growth conditions) but electrical coupling (see Table 3) comparable to that of their growth-arrested counterparts. *Dye data are significantly different at $P \leq 0.001$. Electrical-coupling data were obtained using KCl patch solution; data from growth-arrested and proliferating cells were not different.

Table 3. *Predicted and measured g_j for growth-arrested and proliferating A7r5 cells*

	Proliferating Cells	Growth-Arrested Cells
PS-KCl (g_j = 15.97 mS/cm)	19.6 ± 1.5 (12)	19.7 ± 1.8 (13)
PS-KGlut (g_j = 11.75 mS/cm)	18 ± 1* (14)	14.4 ± 1 (10)
Predicted 26% decline in g_j	14.7	14.7
PS-TEACl (g_j = 10.77 mS/cm)	16.6 ± 1* (17)	14.1 ± 1.4 (13)
Predicted 32% decline in g_j	13.4	13.5

Values are means ± SE of number of cell pairs in parentheses, expressed in nS. g_j, junctional conductance. *Significantly different from predicted value ($P < 0.002$ or 0.001).

different from the values predicted by the conductivities of the patch solutions (Fig. 6, Table 3). With PS-KGlut, g_j in proliferating cells was 92% of that measured with PS-KCl compared with the predicted 74% ($P < 0.002$, measured vs. predicted). Conductance was also higher than predicted when K^+ was replaced with TEA^+: 85% vs. the predicted 67% ($P < 0.001$). These data suggest that in proliferating cells *1*) K^+ and Cl^- contribute nearly equally (some preference for cations) to macroscopic junctional current, whereas TEA^+ and $Glut^-$ do not contribute significantly to junctional current, *2*) at the level of the individual channel, current is carried by only one ion at a time, and *3*) the contribution of K^+ and Cl^-, but not $Glut^-$ or TEA^+, to junctional current is predicted by their mobilities in bulk solution.

DISCUSSION

To better appreciate the potential role of gap junctions in growth properties of cells, the permeability of the junctions to molecules with growth-regulatory po-

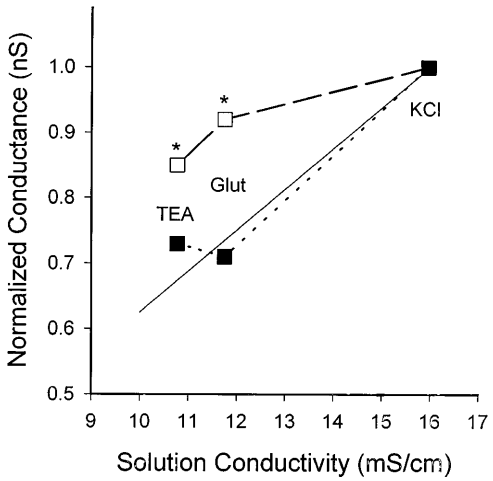

Fig. 6. Junctional conductance of growth-arrested (■) and proliferating (□) cells measured with KCl, potassium glutamate (Glut), and tetraethylammonium chloride (TEA) patch solutions (PS-KCl, PS-KGlut, PS-TEACl) was normalized to PS-KCl. Data are from Table 3. Solid line, junctional conductance if permeation is determined by solution conductivity. Junctional conductances for growth-arrested cells are well predicted by solution conductivities: PS-KGlut and PS-TEACl were not different from values predicted by solution conductivities. *Significantly higher than predicted from solution conductivities.

tential must be elucidated. The purpose of the present study was to characterize functional differences in macroscopic permeability of gap junctions between growth-arrested and proliferating A7r5 cells. We demonstrate that these cells do not proliferate and reside largely in the G_0/G_1 phase of the cell cycle when maintained in media with low serum content. The g_j values, when measured with a KCl pipette solution, were equal in growth-arrested and proliferating cells, suggesting that electrical signals are shared equally well in both growth conditions. However, permeation of the junctions by large ions of either charge was restricted in proliferating cells, suggesting that metabolic and chemical signaling may be compromised in proliferating cells. These observations are discussed with respect to their possible mechanistic basis and their potential implications for growth control.

The dye-coupling studies presented here suggested that gap junctions in proliferating A7r5 cells were less well permeated by Lucifer yellow than their counterparts in growth-arrested cells. The decreased dye coupling in proliferating cells could occur as a result of *1*) decreased activity or numbers of channels with selectivity comparable to those in growth-arrested cells, *2*) decreased anion permeability with or without changes in cation permeability, *3*) decreased large molecule permeability, irrespective of molecular charge, *4*) decreased numbers of contacting cells, or *5*) increased cytosolic expression of dye-binding proteins (8, 34). The pipette solutions used in our studies allowed us to distinguish between these possibilities as follows. If permeation of gap junction channels is dictated largely by the mobility of the current-carrying ions in bulk solution, then differences in g_j measured with the three solutions should be predicted by their conductivities (Fig. 6). If a junction exhibits cation selectivity, then g_j measured with PS-KGlut vs. PS-KCl should differ by less than predicted by their solution conductivities (above solid line in Fig. 6), whereas g_j measured with PS-TEACl vs. PS-KCl should differ by more than predicted by their solution conductivities (below the solid line in Fig. 6). The opposite would be expected for a junction exhibiting anion selectivity. If junctions restrict the movement of large ions, irrespective of their charge, then g_j measured with PS-KGlut and PS-TEACl should differ from that measured with PS-KCl by less than predicted by the respective solution conductivities (above the solid line in Fig. 6). Finally, electrical coupling between growth-arrested and proliferating cells should not differ if dye-coupling data are explained by increased expression of cytosolic dye-binding proteins or decreased numbers of contacting cells in the proliferating cell group. As discussed below and shown in Fig. 6, our data suggest that the junctions in proliferating cells restrict the permeation of large ions, irrespective of their charge.

For growth-arrested cells, g_j values measured with PS-KCl, PS-KGlut, and PS-TEACl were well predicted by solution conductivities, consistent with the conclusion that permeation of gap junction channels in growth-arrested cells is dictated in large part by the mobilities of the ions in bulk solution. The data further suggest that anions and cations permeate the junction equally well and simultaneously (Fig. 7*A*). Thus these junctions exhibit the nonselective behavior stereotypically described for gap junctions in most textbooks. Very different conclusions are required to explain results obtained with proliferating cells.

In proliferating cells, g_j measured with PS-KGlut vs. PS-KCl differed by only 8% rather than the predicted 26%. In the absence of additional information, these data would suggest that gap junctions in proliferating cells exhibit significant cation selectivity. However, g_j measurements with PS-TEACl vs. PS-KCl differed by only 15% rather than the predicted 32%, which would seem to suggest that gap junctions exhibit significant anion selectivity. Together, these data indicate that gap junction channels in proliferating cells restrict the movement of larger molecules irrespective of their charge but are permeated equally well (slight preference for cations) but not simultaneously by small anions and cations (Fig. 7*B*). Thus the data indicate that decreased dye coupling in proliferating vs. growth-arrested cells results from diminished permeation by large molecules irrespective of their charge.

Macroscopic junctional selectivity represents the summation of the selectivities of all the individual channels in the junction. The permselectivity characteristics for Cx40 and Cx43 channels have been published (1, 36, 39), although a clear picture has yet to emerge. On the

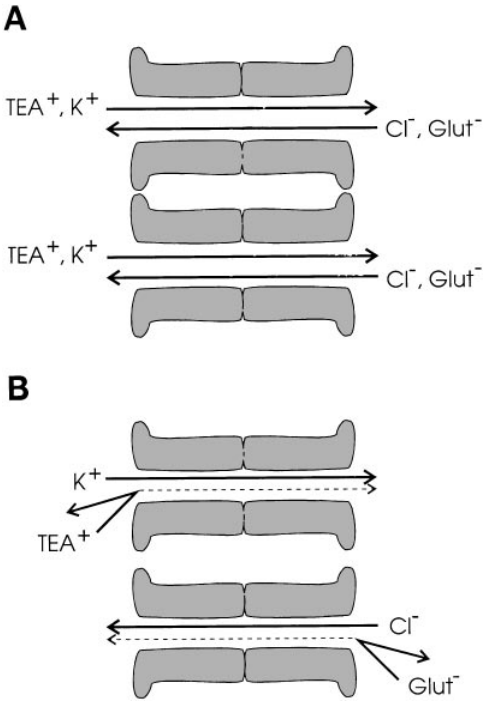

Fig. 7. Model of how junctions between growth-arrested and proliferating cells might behave in face of a transjunctional potential difference. Note simultaneous anion and cation currents and permeation by tetraethylammonium (TEA^+) and glutamate ions ($Glut^-$) in growth-arrested cells (*A*) vs. anion or cation current and poor permeation by TEA^+ and $Glut^-$ in proliferating cells (*B*).

basis of reversal potential measurements with asymmetric solutions, Wang and Veenstra (39) concluded that Cl^-/K^+ selectivity of homomeric/homotypic Cx43 channels was 0.13. However, using symmetric solutions, Wang and Veenstra and Valiunas et al. (36) found that the unitary conductance (γ_j) of Cx43 channels in their main state was dictated in large part by the mobility of the current-carrying ions in bulk solution. Valiunas et al. found that γ_j measured with cesium aspartate vs. KCl differed by 64% vs. a solution conductivity difference of 67%. Similarly, Wang and Veenstra found that γ_j measured with KGlut and TEACl were 63 and 55% of the conductance measured with KCl, values reasonably predicted by the mobility of ions in bulk solution. These measurements suggest that the main state of Cx43 channels exhibits nearly equal anion and cation permeability. In contrast, the residual state of the Cx43 channel appears to exhibit significant cation selectivity (36). Cx40 channels exhibit a more restricted permeation pattern. Beblo and Veenstra (1) found that γ_j values measured with KGlut and TEACl were 113 and 44%, respectively, of the conductance measured with KCl. From these and other measurements, they conclude that Cx40 channels exhibit cation selectivity with poor permeation of the channel by large anions. Again, cation permeation was approximated by ion mobility in bulk solution with minor restriction by the channel. Despite the poor permeation of Cx40 channels by anions suggested by these studies, Elfgang and colleagues (13) demonstrated quite convincingly that Lucifer yellow permeates Cx40 channels just as it permeates Cx43 channels. The measurements of Valiunas et al. and Veenstra and colleagues (1, 39) were made on cells exposed to growth factors. No data are available as to how or even whether these permeability properties might be altered by growth status. Nor are there data regarding open probability as a function of growth status.

Are the junctional permeability characteristics described here for the growth-arrested or proliferating cells consistent with what would be expected for cells expressing Cx40 and Cx43? On the basis of the selectivities of homomeric/homotypic Cx40 vs. Cx43 channels reviewed above, at least four scenarios could be consistent with the data. *1*) In proliferating cells, Cx43 might be downregulated and Cx40 upregulated, such that junctional permeability is reduced but electrical coupling maintained in proliferating vs. growth-arrested cells. *2*) Cx43 channels in proliferating cells might be phosphorylated (26), such that their permeation by large molecules is restricted while permeation by small molecules and consequently electrical coupling is maintained. *3*) In proliferating cells the open probability of Cx43 channels might be reduced [practically speaking to zero (9)] with a compensatory increase in open probability of Cx40 channels. *4*) Cx40 and Cx43 could form heteromeric channels (7, 19), the permeation of which by large molecules decreases as the contribution of Cx40 to the channel increases. In this case, any change in connexin expression that resulted in an increased ratio of Cx40 to Cx43 in the proliferating cells would result in restricted permeation, possibly without major changes in electrical coupling. Further studies are necessary to resolve these possibilities.

The dye-coupling and permselectivity data presented here indicate that growth-arrested cells share large molecules much more readily than their proliferating counterparts. Large molecules of potential interest to cells include metabolites and second messengers (e.g., inositol trisphosphate, cAMP, cGMP). Focusing on the latter, our data suggest that these molecules would diffuse readily between growth-arrested cells but poorly between proliferating cells. Given the short half-life of second-messenger molecules, the limited diffusion of large molecules observed in the proliferating setting may functionally restrict second-messenger molecules to the cells in which they are being actively generated. The significance of such a restriction depends on whether the gap junction serves a growth-suppressing or -promoting role in the cell type being studied.

In a growth-promoting role, growth factors are envisioned to induce a rise in second-messenger concentration that is sufficient to trigger a growth response in the stimulated cell as well as in neighboring cells to which the stimulated cell is coupled. In a growth-suppressing role (23), a growth factor-induced rise in second-messenger levels fails to reach a critical growth-inducing concentration in the stimulated cell, because the molecule rapidly diffuses to neighboring cells (thereby diluting the signal). Our data suggest that in growth-arrested vascular SMCs, at least those expressing Cx40 and Cx43, the gap junction plays a suppressive role, wherein a rise in concentration of a potential growth-regulatory molecule is diluted out because of significant intercellular coupling, effectively shifting the dose-response curve for the growth factor to the right. At sufficiently high growth factor concentration, proliferation is triggered, despite high levels of coupling, perhaps as a consequence of transient uncoupling (21, 29). Maintenance of the proliferating state would then be facilitated by gap junctions that restrict diffusion of growth-regulatory molecules away from the stimulated cell, thereby ensuring sufficient concentration of those molecules for proliferation to continue.

In summary, whereas electrical signaling is preserved, chemical and metabolic signaling is compromised in proliferating A7r5 cells. These results suggest that vasomotor control should be maintained in vascular smooth muscle stimulated to proliferate, as in vasculogenesis, angiogenesis, injury, and disease. It will be interesting to determine whether the proliferation-induced changes in communication described here are unique to A7r5 cells or smooth muscle cells, common to cells coexpressing Cx40 and Cx43, or generic to proliferating vs. growth-arrested cells irrespective of connexin expression.

This work was supported by National Heart, Lung, and Blood Institute Institutional Training Grant 2T32 HL-07249 and Grants HL-31008 and HL-58732 and by Arizona Disease Control Research Commission Grant 5-090.

Present address of D. T. Kurjiaka: Dept. of Biological Sciences, Ohio University, Athens, OH 45701.

Address for reprint requests: J. M. Burt, Dept. of Physiology, University of Arizona, PO Box 245051, Tucson, AZ 85724-5051.

Received 5 March 1998; accepted in final form 27 August 1998.

REFERENCES

1. **Beblo, D. A., and R. D. Veenstra.** Monovalent cation permeation through the connexin40 gap junction channel Cs, Rb, K, Na, Li, TEA, TMA, TBA, and effects of anions Br, Cl, F, acetate, aspartate, glutamate, and NO_3. *J. Gen. Physiol.* 109: 509–522, 1997.
2. **Bennett, M. R., G. I. Evan, and A. C. Newby.** Deregulated expression of the c-*myc* oncogene abolishes inhibition of proliferation of rat vascular smooth cells by serum reduction, interferon-γ, heparin, and cyclic nucleotide analogues and induces apoptosis. *Circ. Res.* 74: 525–536, 1994.
3. **Bennett, M. R., T. D. Littlewood, D. C. Hancock, G. I. Evan, and A. C. Newby.** Down-regulation of the c-*myc* proto-oncogene in inhibition of vascular smooth-muscle cell proliferation: a signal for growth arrest? *Biochem. J.* 301: 702–708, 1994.
4. **Beyer, E. C., K. E. Reed, E. M. Westphale, H. L. Kanter, and D. M. Larson.** Molecular cloning and expression of rat connexin40, a gap junction protein expressed in vascular smooth muscle. *J. Membr. Biol.* 127: 69–76, 1992.
5. **Blackburn, J. P., J. L. Connat, N. J. Severs, and C. R. Green.** Connexin43 gap junction levels during development of the thoracic aorta are temporally correlated with elastic laminae deposition and increased blood pressure. *Cell Biol. Int.* 21: 87–97, 1997.
6. **Blackburn, J. P., N. S. Peters, H.-I. Yeh, S. Rothery, C. R. Green, and N. J. Severs.** Upregulation of connexin43 gap junctions during early stages of human coronary atherosclerosis. *Arterioscler. Thromb. Vasc. Biol.* 15: 1219–1228, 1995.
7. **Brink, P. R., K. Cronin, K. Banach, E. Peterson, E. M. Westphale, K. H. Seul, S. V. Ramanan, and E. C. Beyer.** Evidence for heteromeric gap junction channels formed from rat connexin43 and human connexin37. *Am. J. Physiol.* 273 (*Cell Physiol.* 42): C1386–C1396, 1997.
8. **Brink, P. R., and S. V. Ramanan.** A model for the diffusion of fluorescent probes in the septate giant axon of earthworm. Axoplasmic diffusion and junctional membrane permeability. *Biophys. J.* 48: 299–309, 1985.
9. **Brink, P. R., S. V. Ramanan, and G. J. Christ.** Human connexin 43 gap junction channel gating: evidence for mode shifts and/or heterogeneity. *Am. J. Physiol.* 271 (*Cell Physiol.* 40): C321–C331, 1996.
10. **Bruzzone, R., T. W. White, and D. L. Paul.** Connections with connexins: the molecular basis of direct intercellular signaling. *Eur. J. Biochem.* 238: 1–27, 1996.
11. **Christ, G. J., D. C. Spray, M. E. El-Sabban, L. K. Moore, and P. R. Brink.** Gap junctions in vascular tissues: role of heterotypic and homotypic intercellular communication in the modulation of vasomotor tone. *Circ. Res.* 79: 631–646, 1996.
12. **Doble, B. W., Y. Chen, D. G. Bosc, D. W. Litchfield, and E. Kardami.** Fibroblast growth factor-2 decreases metabolic coupling and stimulates phosphorylation as well as masking of connexin43 epitopes in cardiac myocytes. *Circ. Res.* 79: 647–658, 1996.
13. **Elfgang, C., R. Eckert, H. Lichtenberg-Frate, A. Butterweck, O. Traub, R. A. Klein, D. Hulser, and K. Willecke.** Specific permeability and selective formation of gap junction channels in connexin-transfected HeLa cells. *J. Cell Biol.* 129: 805–817, 1995.
14. **Gibbons, G. H., R. E. Pratt, and V. J. Dzau.** Vascular smooth muscle cell hypertrophy vs. hyperplasia. Autocrine transforming growth factor-β_1 expression determines growth response to angiotensin II. *J. Clin. Invest.* 90: 456–461, 1992.
15. **Grunwald, J., H. Robenek, J. Mey, and W. H. Hauss.** In vivo and in vitro cellular changes in experimental hypertension: electronmicroscopic and morphometric studies of aortic smooth muscle cells. *Exp. Mol. Pathol.* 36: 164–176, 1982.
16. **Haefliger, J. A., E. Castillo, G. Waeber, G. E. Bergonzelli, J. F. Aubert, E. Sutter, P. Nicod, B. Waeber, and P. Meda.** Hypertension increases connexin43 in a tissue-specific manner. *Circulation* 95: 1007–1014, 1997.
17. **Hatch, F. T., and R. S. Lees.** Practical methods for plasma lipoprotein analysis. *Adv. Lipid Res.* 6: 1–68, 1968.
18. **Havel, R. J., H. A. Eder, and J. H. Bragdon.** The distribution and chemical composition of ultracentrifugally separated lipoproteins in human serum. *J. Clin. Invest.* 34: 1345–1353, 1955.
19. **He, D. S., and J. M. Burt.** Function of gap junction channels formed in cells co-expressing connexins 40 and 43. In: *Gap Junctions*, edited by R. Werner. Amsterdam: IOS, 1998, p. 40–44.
20. **Larson, D. M., M. J. Wrobleski, G. D. V. Sagar, E. M. Westphale, and E. C. Beyer.** Differential regulation of connexin43 and connexin37 in endothelial cells by cell density, growth, and TGF-β_1. *Am. J. Physiol.* 272 (*Cell Physiol.* 41): C405–C415, 1997.
21. **Lau, A. F., M. Y. Kanemitsu, W. E. Kurata, S. Danesh, and A. L. Boynton.** Epidermal growth factor disrupts gap junctional communication and induces phosphorylation of connexin43 on serine. *Mol. Biol. Cell* 3: 865–874, 1992.
22. **Little, T. L., E. C. Beyer, and B. R. Duling.** Connexin43 and connexin40 gap junctional proteins are present in both arteriolar smooth muscle and endothelium in vivo. *Am. J. Physiol.* 268 (*Heart Circ. Physiol.* 37): H729–H739, 1995.
23. **Loewenstein, W. R.** Junctional intercellular communication and the control of growth. *Biochim. Biophys. Acta* 560: 1–65, 1979.
24. **Moore, L. K., E. C. Beyer, and J. M. Burt.** Characterization of gap junction channels in A7r5 vascular smooth muscle cells. *Am. J. Physiol.* 260 (*Cell Physiol.* 29): C975–C981, 1991.
25. **Moore, L. K., and J. M. Burt.** Gap junction function in vascular smooth muscle: influence of serotonin. *Am. J. Physiol.* 269 (*Heart Circ. Physiol.* 38): H1481–H1489, 1995.
26. **Moreno, A. P., J. C. Saez, G. I. Fishman, and D. C. Spray.** Human connexin43 gap junction channels: regulation of unitary conductances by phosphorylation. *Circ. Res.* 74: 1050–1057, 1994.
27. **Nilsson, J., M. Sjolund, L. Palmberg, J. Thyberg, and C. H. Heldin.** Arterial smooth muscle cells in primary culture produce a platelet-derived growth factor-like protein. *Proc. Natl. Acad. Sci. USA* 82: 4418–4422, 1985.
28. **Ozer, N. K., P. Palozza, D. Boscoboinik, and A. Azzi.** *d*-α-Tocopherol inhibits low density lipoprotein induced proliferation and protein kinase C activity in vascular smooth muscle cells. *FEBS Lett.* 322: 307–310, 1993.
29. **Pelletier, D. B., and A. L. Boynton.** Dissociation of PDGF receptor tyrosine kinase activity from PDGF-mediated inhibition of gap junctional communication. *J. Cell. Physiol.* 158: 427–434, 1994.
30. **Pepper, M. S., R. Montesano, A. El Aoumari, D. Gros, L. Orci, and P. Meda.** Coupling and connexin 43 expression in microvascular and large vessel endothelial cells. *Am. J. Physiol.* 262 (*Cell Physiol.* 31): C1246–C1257, 1992.
31. **Segal, S. S., and B. R. Duling.** Conduction of vasomotor responses in arterioles: a role for cell-to-cell coupling? *Am. J. Physiol.* 256 (*Heart Circ. Physiol.* 25): H838–H845, 1989.
32. **Segal, S. S., and D. T. Kurjiaka.** Coordination of blood flow control in the resistance vasculature of skeletal muscle. *Med. Sci. Sports Exerc.* 27: 1158–1164, 1997.
33. **Sneyd, J., B. T. R. Wetton, A. C. Charles, and M. J. Sanderson.** Intercellular calcium waves mediated by diffusion of inositol trisphosphate: a two-dimensional model. *Am. J. Physiol.* 268 (*Cell Physiol.* 37): C1537–C1545, 1995.
34. **Stewart, W. W.** Functional connections between cells as revealed by dye-coupling with a highly fluorescent naphthalimide tracer. *Cell* 14: 741–759, 1978.
35. **Tsai, M. L., S. W. Watts, R. Loch-Caruso, and R. C. Webb.** The role of gap junctional communication in contractile oscillations in arteries from normotensive and hypertensive rats. *J. Hypertens.* 13: 1123–1133, 1995.

36. **Valiunas, V., F. Bukauskas, and R. Weingart.** Conductances and selective permeability of connexin43 gap junction channels examined in neonatal rat heart cells. *Circ. Res.* 80: 708–719, 1997.
37. **Van Rijen, H. V. M., R. Wilders, A. C. G. Van Ginneken, and H. J. Jongsma.** Quantitative analysis of dual whole-cell voltage-clamp determination of gap junctional conductance. *Pflügers Arch.* 436: 141–151, 1998.
38. **Vindelov, L. L., and I. J. Christensen.** Detergent and proteolytic enzyme-based techniques for nuclear isolation and DNA content analysis. In: *Flow Cytometry*, edited by Z. Darzynkiewicz, J. P. Robinson, and H. A. Crissman. San Diego, CA: Academic, 1994, p. 219–229.
39. **Wang, H.-Z., and R. D. Veenstra.** Monovalent ion selectivity sequences of the rat connexin43 gap junction channel. *J. Gen. Physiol.* 109: 491–507, 1997.
40. **Wilders, R., and H. J. Jongsma.** Limitations of the dual voltage clamp method in assaying conductance and kinetics of gap junction channels. *Biophys. J.* 63: 942–953, 1992.
41. **Winkles, J. A., R. Friesel, W. H. Burgess, R. Howk, T. Mehlman, R. Weinstein, and T. Maciag.** Human vascular smooth muscle cells both express and respond to heparin-binding growth factor I (endothelial cell growth factor). *Proc. Natl. Acad. Sci. USA* 84: 7124–7128, 1987.
42. **Yamasaki, H., and C. C. G. Naus.** Role of connexin genes in growth control. *Carcinogenesis* 17: 1199–1213, 1996.